

This material has been copied  
under licence from CANCOPY.  
Resale or further copying of this material is  
strictly prohibited.

Le présent document a été reproduit  
avec l'autorisation de CANCOPY.  
La revendre ou la reproduction ultérieure  
en sont strictement interdites.

NUCLEAR SCIENCE AND ENGINEERING: 62, 559-570 (1977)

## Reactivity Worths of Annular Control Rods in a Pressure-Tube-Type Heavy Water Lattice

Makoto Ueda\* and Mitsuo Matsumoto

Power Reactor and Nuclear Fuel Development Corporation  
1-9-13 Akasaka, Minato-ku, Tokyo, Japan

and

Tohru Haga<sup>†</sup>

Atomic Energy Research Laboratory, Hitachi Ltd., Ozenji, Kawasaki-shi, Japan

Received December 2, 1975

Revised September 22, 1976

The control rod effect has been experimentally studied in the Deuterium Critical Assembly (DCA) by using annular absorbers that simulate control rods of the FUGEN reactor, a prototype heavy-water-moderated, boiling-light-water-cooled, pressure-tube-type reactor. The DCA cores for this experiment are of the 1.2% <sup>235</sup>U-enriched UO<sub>2</sub> lattices, and consist of 28-pin fuel clusters arranged in a square array of 22.5-cm lattice pitch. The experiment has been carried out with various control rod patterns and with varying coolant void fraction.

Experimental results were analyzed by the "absorption area method," which was employed in the FUGEN control rod design calculations. The calculated reactivity worth agreed with the experiment within  $\pm 10\%$ . The calculations somewhat overestimated the absorber worths in the nonvoided core and underestimated them in the voided core. This tendency was found to be greatly improved by considering the anisotropy effect in the migration area of the cluster lattice. The experimental results were also analyzed by the "logarithmic derivative method." This method more poorly predicted the worths, but described better the flux shape around the rods.

### I. INTRODUCTION

FUGEN (Ref. 1) is a heavy-water-moderated, boiling-light-water-cooled, pressure-tube-type reactor. For reactivity control of this reactor, 49 annular control rods (CRs) are to be used. A series of critical experiments was performed in the Deuterium Critical Assembly<sup>2</sup> (DCA)

to study the physics of a heavy-water-moderated, pressure-tube-type reactor lattice.

For the design calculation of the CR effect, a simple calculational technique is more desirable as long as it is reasonably accurate. The method adopted in the design calculation of the FUGEN CR is the "absorption area method" (AA method).<sup>3-5</sup> This method was independently considered for the FUGEN CR analysis, but it was later found to be equivalent to the one developed by Greebler.<sup>4</sup>

The direct full-core diffusion calculation was also employed as an alternative, applying the logarithmic-derivative condition at the CR surface (LD method). In this paper, the details on the CR experiments are presented together with the calculations made by the two methods.

\*Present address: NAIG Nuclear Research Laboratory, Nippon Atomic Industry Group Co., 4-1 Ukishima-cho, Kawasaki-shi, Japan.

<sup>†</sup>Present address: Power Reactor and Nuclear Fuel Development Corporation, 1-9-13 Akasaka, Minato-ku, Tokyo, Japan.

<sup>1</sup>S. SHIMA, S. NAKATA, and S. SAWAI, "Development of Prototype Heavy Water Reactor (FUGEN) in Japan," *Proc. 4th Int. Conf. Peaceful Uses At. Energy*, 5, 283 (1971).

<sup>2</sup>Y. MIYAWAKI and H. KATO, "Heavy Water Critical Experiments on Plutonium Utilization in Advanced Thermal Reactor FUGEN," PNC N941 74-72, IAEA Panel on Plutonium Utilization in Thermal Power Reactors, Nov. 25-29, 1974, Karlsruhe, International Atomic Energy Agency (Oct. 1974).

<sup>3</sup>H. HURWITZ, Jr. and G. M. ROE, *J. Nucl. Energy*, 2, 85 (1955).

<sup>4</sup>P. GREEBLER, *Nucl. Sci. Eng.*, 3, 445 (1958).

<sup>5</sup>S. PEARLSTEIN, *Nucl. Sci. Eng.*, 4, 322 (1958).

<sup>6</sup>R. W. DEUTSCH, *Nucl. Sci. Eng.*, 5, 150 (1959).

## II. EXPERIMENT

### II.A. Experimental Facilities

The cross-sectional view of an experimental annular CR is first shown in Fig. 1. The experimental CR consists of small absorber elements assembled in a double annulus of 82-mm o.d. Each absorber element is a stainless-steel tube of  $3.58 \pm 0.03$ -mm i.d. and  $4.75 \pm 0.02$ -mm o.d., containing  $B_4C$  of  $(70 \pm 1)\%$  theoretical density.

The lattice data, fuel cluster, and core layout of the critical assembly are given in Table I and in Figs. 2 and 3, respectively. The cores used for the experiment were of the 1.2%-enriched  $UO_2$  lattices consisting of 28-pin fuel clusters in square arrays with a 22.5-cm pitch. The intermediate coolant voiding, i.e., 30, 70, and 86.7% void conditions, were simulated by adjusting the composition of mixtures of  $H_2O$ ,  $D_2O$ , and  $H_3BO_3$  in such a way as to conserve the slowing down power,  $\xi\Sigma_s$ , and the thermal neutron absorption cross section,  $\Sigma_{a,th}$ .

The CRs were inserted in between the fuel assemblies through the "experimental hole" (see Fig. 3). A maximum of nine experimental absorber rods were inserted.

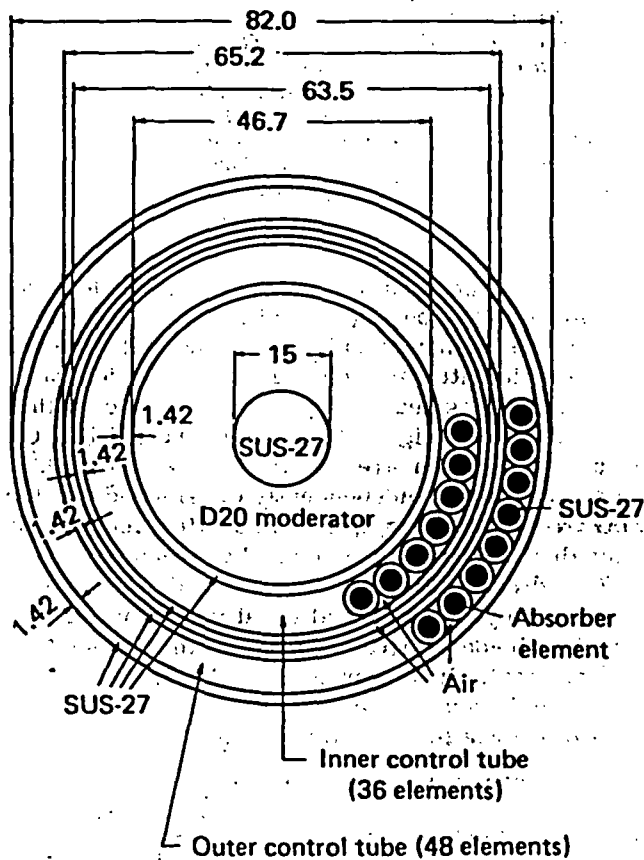


Fig. 1. Cross section of a control rod (all dimensions in mm).

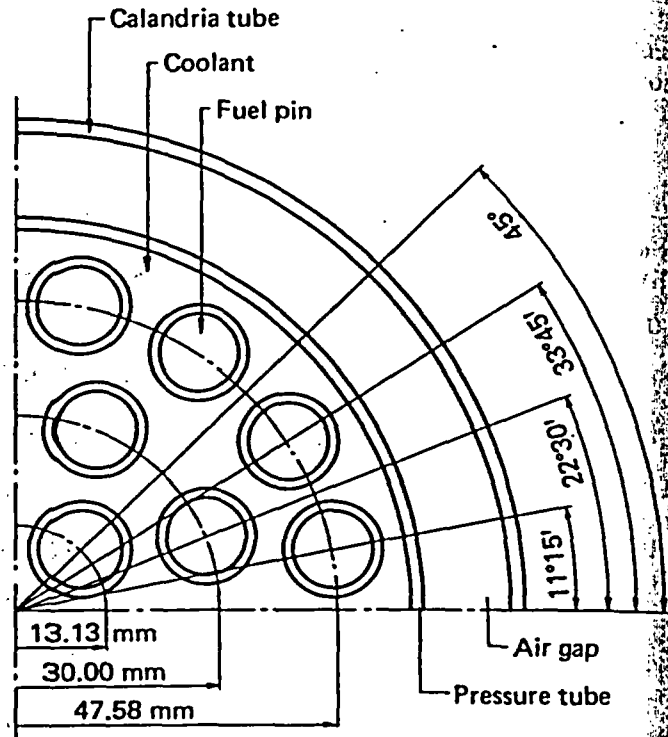


Fig. 2. Fuel cluster.

### II.B. Method of Reactivity Determination

Shown in Fig. 4 is the experimental procedure to determine the reactivity worth of the CRs (CR worth). The worth is obtained by integrating the calibrated moderator-level-worth curve between two critical moderator levels with and without CRs in the core. Note that the critical  $D_2O$ -moderator height is affected by the coolant level in the fuel channel, and therefore the critical height is always adjusted to the condition of equal moderator and coolant heights. The reactivity coefficient of the water level,  $\partial\rho/\partial h$ , was measured by a positive-period method. The  $\partial\rho/\partial h$  value is slightly affected by the CR strength (see Sec. II.D) and also by the moderator-minus-coolant level difference (MCD). The MCD effect on  $\partial\rho/\partial h$  was, in most cases, negligible under the experimental condition such that  $|MCD| \leq 15$  cm. This was also examined by a one-dimensional diffusion calculation.

### II.C. Critical Buckling, $B_0^2$

The relationship between MCD and observed critical moderator height was studied experimentally. In most measurements, the MCD value was in the range from -15 to +15 cm, and this required a correction of the observed critical moderator height in the range from +1.0 to -2.0 cm.

TABLE I  
DCA Lattice Data

| Region   | Descriptions   |  |                                |     |                              |  |  |                           |            |  |  |  |                              |                  |                  |                                |     |   |     |   |   |   |        |    |      |      |        |   |       |    |      |      |        |   |       |      |      |       |   |   |        |     |   |   |   |     |   |
|--|--|--|--------------------------------|-----|------------------------------|--|--|---------------------------|------------|--|--|--|------------------------------|------------------|------------------|--------------------------------|-----|---|-----|---|---|---|--------|----|------|------|--------|---|-------|----|------|------|--------|---|-------|------|------|-------|---|---|--------|-----|---|---|---|-----|---|
| Cluster  | Diam: 11.68 cm, total number: 121<br>Pellet: $\text{UO}_2$ , 10.357 g/cm <sup>3</sup> , 1.48-cm diam,<br>1.204 wt% <sup>235</sup> U-enriched uranium<br>Clad: Aluminum (Type JIS A2T1), 1.673-cm o.d., 0.85 cm thick<br>Radii of fuel rings: 13.13, 30.00, and 47.58 mm<br>Coolant: $\text{H}_2\text{O}$ , $\text{H}_2\text{O} + \text{D}_2\text{O} + \text{H}_3\text{BO}_3$ (mixtures), 99.50 mol% $\text{D}_2\text{O}$ , or air<br><table border="1" style="margin: 10px auto;"> <thead> <tr> <th colspan="6">Ingredient and Density of Void-Simulated Coolant</th> </tr> <tr> <th rowspan="2">Coolant Void Fraction (%)</th> <th colspan="4">Weight (%)</th> <th rowspan="2">Density (g/cm<sup>3</sup>)</th> </tr> <tr> <th>H<sub>2</sub>O</th> <th>D<sub>2</sub>O</th> <th>H<sub>3</sub>BO<sub>3</sub></th> <th>Air</th> </tr> </thead> <tbody> <tr> <td>0</td> <td>100</td> <td>0</td> <td>0</td> <td>0</td> <td>0.9981</td> </tr> <tr> <td>30</td> <td>63.2</td> <td>36.8</td> <td>0.0092</td> <td>0</td> <td>1.036</td> </tr> <tr> <td>70</td> <td>18.1</td> <td>81.9</td> <td>0.0215</td> <td>0</td> <td>1.087</td> </tr> <tr> <td>86.7</td> <td>0.47</td> <td>99.53</td> <td>0</td> <td>0</td> <td>1.1048</td> </tr> <tr> <td>100</td> <td>0</td> <td>0</td> <td>0</td> <td>100</td> <td>0</td> </tr> </tbody> </table> | Ingredient and Density of Void-Simulated Coolant |                                |     |                              |  |  | Coolant Void Fraction (%) | Weight (%) |  |  |  | Density (g/cm <sup>3</sup> ) | H <sub>2</sub> O | D <sub>2</sub> O | H <sub>3</sub> BO <sub>3</sub> | Air | 0 | 100 | 0 | 0 | 0 | 0.9981 | 30 | 63.2 | 36.8 | 0.0092 | 0 | 1.036 | 70 | 18.1 | 81.9 | 0.0215 | 0 | 1.087 | 86.7 | 0.47 | 99.53 | 0 | 0 | 1.1048 | 100 | 0 | 0 | 0 | 100 | 0 |
| Ingredient and Density of Void-Simulated Coolant |  |  |                                |     |                              |  |  |                           |            |  |  |  |                              |                  |                  |                                |     |   |     |   |   |   |        |    |      |      |        |   |       |    |      |      |        |   |       |      |      |       |   |   |        |     |   |   |   |     |   |
| Coolant Void Fraction (%)                        | Weight (%)   |  |                                |     | Density (g/cm <sup>3</sup> ) |  |  |                           |            |  |  |  |                              |                  |                  |                                |     |   |     |   |   |   |        |    |      |      |        |   |       |    |      |      |        |   |       |      |      |       |   |   |        |     |   |   |   |     |   |
|  | H <sub>2</sub> O   | D <sub>2</sub> O                                 | H <sub>3</sub> BO <sub>3</sub> | Air |                              |  |  |                           |            |  |  |  |                              |                  |                  |                                |     |   |     |   |   |   |        |    |      |      |        |   |       |    |      |      |        |   |       |      |      |       |   |   |        |     |   |   |   |     |   |
| 0  | 100  | 0  | 0                              | 0   | 0.9981                       |  |  |                           |            |  |  |  |                              |                  |                  |                                |     |   |     |   |   |   |        |    |      |      |        |   |       |    |      |      |        |   |       |      |      |       |   |   |        |     |   |   |   |     |   |
| 30   | 63.2   | 36.8   | 0.0092                         | 0   | 1.036                        |  |  |                           |            |  |  |  |                              |                  |                  |                                |     |   |     |   |   |   |        |    |      |      |        |   |       |    |      |      |        |   |       |      |      |       |   |   |        |     |   |   |   |     |   |
| 70   | 18.1   | 81.9   | 0.0215                         | 0   | 1.087                        |  |  |                           |            |  |  |  |                              |                  |                  |                                |     |   |     |   |   |   |        |    |      |      |        |   |       |    |      |      |        |   |       |      |      |       |   |   |        |     |   |   |   |     |   |
| 86.7   | 0.47   | 99.53  | 0                              | 0   | 1.1048                       |  |  |                           |            |  |  |  |                              |                  |                  |                                |     |   |     |   |   |   |        |    |      |      |        |   |       |    |      |      |        |   |       |      |      |       |   |   |        |     |   |   |   |     |   |
| 100  | 0  | 0  | 0                              | 100 | 0                            |  |  |                           |            |  |  |  |                              |                  |                  |                                |     |   |     |   |   |   |        |    |      |      |        |   |       |    |      |      |        |   |       |      |      |       |   |   |        |     |   |   |   |     |   |
| Pressure tube                                    | 12.08-cm o.d., 0.2 cm thick, aluminum (Type JIS A2T1)  |  |                                |     |                              |  |  |                           |            |  |  |  |                              |                  |                  |                                |     |   |     |   |   |   |        |    |      |      |        |   |       |    |      |      |        |   |       |      |      |       |   |   |        |     |   |   |   |     |   |
| Air gap  | 13.25-cm o.d.  |  |                                |     |                              |  |  |                           |            |  |  |  |                              |                  |                  |                                |     |   |     |   |   |   |        |    |      |      |        |   |       |    |      |      |        |   |       |      |      |       |   |   |        |     |   |   |   |     |   |
| Calandria tube                                   | 13.65-cm o.d., 0.2 cm thick, aluminum (Type JIS A2T1)  |  |                                |     |                              |  |  |                           |            |  |  |  |                              |                  |                  |                                |     |   |     |   |   |   |        |    |      |      |        |   |       |    |      |      |        |   |       |      |      |       |   |   |        |     |   |   |   |     |   |
| Moderator  | 99.50 mol% $\text{D}_2\text{O}$ , 1.1048 g/cm <sup>3</sup> (20°C)  |  |                                |     |                              |  |  |                           |            |  |  |  |                              |                  |                  |                                |     |   |     |   |   |   |        |    |      |      |        |   |       |    |      |      |        |   |       |      |      |       |   |   |        |     |   |   |   |     |   |
| Lattice  | Square arrays spaced at 22.5 cm  |  |                                |     |                              |  |  |                           |            |  |  |  |                              |                  |                  |                                |     |   |     |   |   |   |        |    |      |      |        |   |       |    |      |      |        |   |       |      |      |       |   |   |        |     |   |   |   |     |   |
| Core tank  | 300.5-cm i.d., 1.0 cm thick, aluminum (Type JIS A2P1)  |  |                                |     |                              |  |  |                           |            |  |  |  |                              |                  |                  |                                |     |   |     |   |   |   |        |    |      |      |        |   |       |    |      |      |        |   |       |      |      |       |   |   |        |     |   |   |   |     |   |
| Grid plates                                      | Upper and lower, aluminum (Type JIS A2P1)  |  |                                |     |                              |  |  |                           |            |  |  |  |                              |                  |                  |                                |     |   |     |   |   |   |        |    |      |      |        |   |       |    |      |      |        |   |       |      |      |       |   |   |        |     |   |   |   |     |   |
| Lower absorber plate                             | $\text{B}_4\text{C}$ + aluminum (thermally black)  |  |                                |     |                              |  |  |                           |            |  |  |  |                              |                  |                  |                                |     |   |     |   |   |   |        |    |      |      |        |   |       |    |      |      |        |   |       |      |      |       |   |   |        |     |   |   |   |     |   |
| Temperature                                      | Room temperature: 20°C   |  |                                |     |                              |  |  |                           |            |  |  |  |                              |                  |                  |                                |     |   |     |   |   |   |        |    |      |      |        |   |       |    |      |      |        |   |       |      |      |       |   |   |        |     |   |   |   |     |   |

The reflector saving in the axial direction, i.e.,  $\delta$  value, was obtained by the least-squares fit of the copper wire activation to a sine function. A number of copper wires were irradiated at the center of both fuel clusters and moderator space. The least-squares fitting was made by a "peeling-off technique," and it was found that  $\delta$  approached an asymptotic value when activation data within 10 cm of the core boundaries (top and bottom) were excluded from the fitting. Measurement showed that the  $\delta$  value in the fuel cluster,  $\delta_F$ , was slightly larger than that in the moderator,  $\delta_M$ , i.e., by  $\sim 1$  to 3 cm in the nonvoided and in the 30%-voided lattices. Strictly speaking, this phenomenon indicates a difficulty in evaluating  $\delta$  values in a homogeneous treatment. A simple

method was employed here to obtain the average  $\delta$  value for practical purposes. Assuming the vacuum boundary condition (as is nearly the case of the DCA core), one has

$$\left. \begin{aligned} \delta_F &= 0.71/\Sigma_{trF} \\ \delta_M &= 0.71/\Sigma_{trM} \\ \delta &= 0.71/\Sigma_{tr} \\ \Sigma_{tr} &= [\Sigma_{trF}(V\phi)_F + \Sigma_{trM}(V\phi)_M]/[(V\phi)_F + (V\phi)_M] \end{aligned} \right\}, (1)$$

where  $\Sigma_{trF}$  and  $\Sigma_{trM}$  are the transport cross sections in each medium,  $\Sigma_{tr}$  is the cell-average transport cross section, and  $(V\phi)_F$  and  $(V\phi)_M$  are the volume integrals of the thermal flux in a fuel

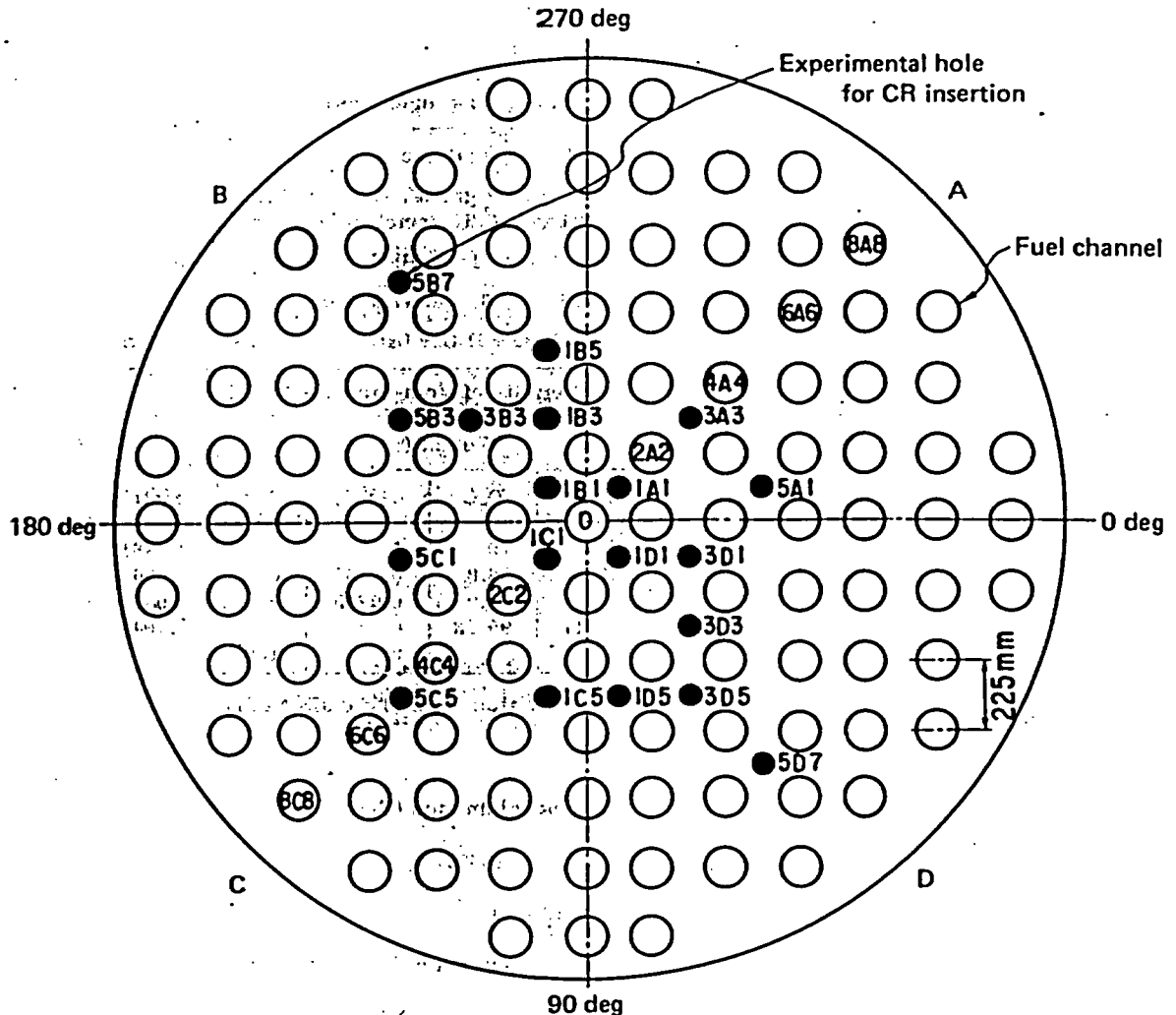
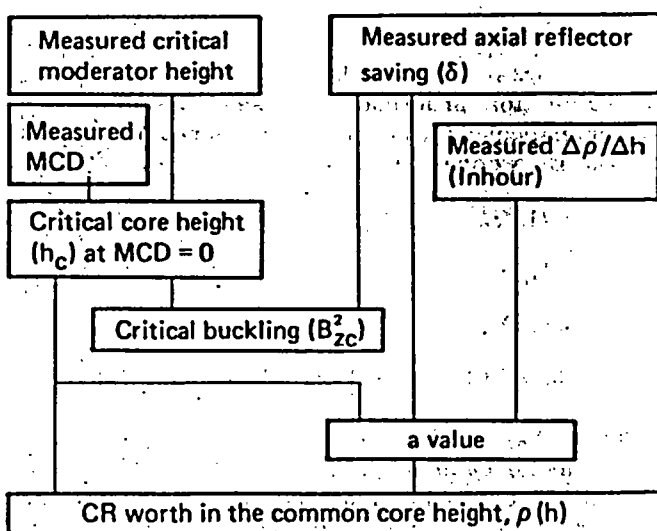


Fig. 3. Core layout showing the location of the experimental control rod.



channel and in the moderator. The cell-averaged  $\delta$  is then given by

$$\delta = \left[ 1 + \frac{(V\phi)_M}{(V\phi)_F} \right] / \left[ \frac{1}{\delta_F} + \frac{1}{\delta_M} \cdot \frac{(V\phi)_M}{(V\phi)_F} \right] \quad (2)$$

Since the values of  $\delta_F$ ,  $\delta_M$ , and  $\delta$  were influenced by the MCD value, the measured  $\delta_F$ ,  $\delta_M$ , and  $\delta$  were always corrected to the MCD = 0 condition, and the results are shown in Table II. Experimental uncertainty of  $\delta$  values was estimated to be within  $\pm 0.5$  cm. The uncertainty resulting from the application of Eq. (2) was not considered. The values of  $\delta_F$  and  $\delta_M$  were insensitive to the presence of the CRs.

Fig. 4. Procedure for reactivity measurement. MCD is the level difference between moderator and coolant, and the  $a$  value =  $(\Delta\rho/\Delta h)(h_c + \delta)^2$ .

TABLE II  
Axial Reflector Saving and  $a$  Value

| Coolant Void Fraction (%) | Axial Reflector Saving (cm) | $a$ Value <sup>a</sup> ( $10^{-2}$ cents $\cdot$ m <sup>2</sup> ) | Measured Range of Axial Buckling, $B_z^2$ (m <sup>-2</sup> ) |
|---------------------------|-----------------------------|---|--|
| 0                         | 10.5                        | 39.6  | 4 - 9  |
| 30                        | 11.2                        | 39.8  | 5.4 - 8.2  |
| 70                        | 11.8                        | $53.2 - 0.788 B_z^2(h_c^A)$                                       | 4.7 - 7.6  |
| 86.7                      | 12.4 <sup>b</sup>           | 59.1  | 7.1 - 7.4  |
| 100                       | 13.8                        | $78.0 - 1.31 B_z^2(h_c^A)$  | 2.4 - 6.2  |

<sup>a</sup>For the buckling dependence of the  $a$  value, see Sec. II.D.  
<sup>b</sup>Estimated graphically.

The radial buckling in the clean core was also determined from the least-squares fit to a  $J_0$  function of copper wire activation irradiated in the center of both fuel clusters and the moderator. The activation traverse in the moderator space resulted in the same radial buckling as that obtained in the fuel space. The measurements were done for nonvoided and 100%-voided cores, and the value was  $2.40 \pm 0.05$  m<sup>-2</sup> for both cases. Hence, the radial buckling in the clean core was assumed to be independent of the coolant void fraction.

#### II.D. Reactivity Coefficient of Water Level, $\partial\rho/\partial h$

The moderator level coefficient is defined by

$$\frac{\partial\rho}{\partial h} = \frac{1}{\beta_{\text{eff}}} \frac{1}{k_{\text{eff}}^2} \frac{\partial k_{\text{eff}}}{\partial h} \quad (3)$$

The reactivity changes from  $\rho^A$  to  $\rho^0$  due to withdrawal of a CR, and the negative CR worth at core height  $h$  is given by

$$\begin{aligned} \rho(h) &= \rho^0 - \rho^A \\ &= \int_{h_c^0}^h \left(\frac{\partial\rho}{\partial h}\right)^0 dh - \int_{h_c^A}^h \left(\frac{\partial\rho}{\partial h}\right)^A dh \\ &= \int_{h_c^0}^h \left(\frac{\partial\rho}{\partial h}\right)^0 dh - \int_{h_c^A}^h \left[ \left(\frac{\partial\rho}{\partial h}\right)^A - \left(\frac{\partial\rho}{\partial h}\right)^0 \right] dh, \quad (4) \end{aligned}$$

where  $(\partial\rho/\partial h)^A$ ,  $(\partial\rho/\partial h)^0$ ,  $h_c^A$ , and  $h_c^0$  are the reactivity coefficients of moderator level and the critical moderator heights, with and without CRs, respectively.

If the axial buckling is given by  $\pi^2/(h + \delta)^2$ , the two-group treatment of  $\partial\rho/\partial h$  becomes

$$\frac{\partial\rho}{\partial h} = \frac{a}{(h + \delta)^3} \quad (5)$$

and

$$a = \frac{2\pi^2 M_z^2}{\beta_{\text{eff}} k_{\infty 2}^2} \left( 1 + \frac{2\tau L^2}{M^2} B_z^2 \right), \quad (6)$$

where  $M_z^2$  is the migration area in the axial direction, and  $M^2$ ,  $\tau$ , and  $L^2$  are the isotropic values of migration, slowing down, and diffusion areas, respectively (see the Appendix). The  $k_{\infty 2}^*$  is related to  $k_{\text{eff}}$  by the well-known form, i.e.,  $k_{\text{eff}} = k_{\infty 2}^* / [(1 + \tau B^2)(1 + L^2 B^2)]$ , and may be called the "two-group multiplication factor in a finite reactor." The  $k_{\infty 2}^*$ , distinguished from  $k_{\infty}$  by Richey and Oakes<sup>7</sup> and by Ueda,<sup>8</sup> depends slightly on the buckling,  $B^2$ , and the ratio  $k_{\infty 2}^*/k_{\infty}$  ranged between 1.01 and 1.02 in the present cores.<sup>8</sup>

The  $a$  value in Eq. (6) is buckling dependent, and  $M_z^2$  and  $k_{\infty 2}^*$  might be affected by the CR insertion. Consequently, the behavior of  $\partial\rho/\partial h$  with CR insertion was also studied numerically. A two-group, two-dimensional diffusion calculation was performed, and the core-averaged values of  $M^2$  and  $k_{\infty 2}^*$  were obtained with CRs in the core. The  $M^2/k_{\infty 2}^*$ , which is proportional to the  $a$  value, was linearly related to the critical axial buckling  $B_z^2(h_c^A)$ , and the ratio was found to be insensitive to the position of CR insertion. Reactivity worth,  $\Delta\rho$ , of incremental moderator level change,  $\Delta h$ , from the critical height,  $h_c$ , yields the ratio  $\Delta\rho/\Delta h$  at a level of  $h_c + \Delta h/2$  (Ref. 9). The  $a$  values at various critical core heights were fitted to a linear function with respect to  $B_z^2(h_c)$ . Since the experimental value of  $\Delta\rho$  by a positive period method was limited within  $\sim 20$  cents at most, the increment  $\Delta h$  was only in the range from 0.2 to 1.0 cm. This limitation caused an uncertainty of  $\pm 3.5\%$  in the evaluated individual  $a$  values in the worst case, which happened in the clean critical core. The result of the least-squares fit would give more accurate  $a$  values, with an uncertainty of about  $\pm 1.5\%$ .

#### II.E. Results of Reactivity Measurement

The axial critical bucklings,  $B_z^2(h_c^A)$ , together with the CR worths at a fixed buckling,  $B_z^2 = 6.11$  m<sup>-2</sup>, are given in Table III. The maximum correction made to the CR worth was 7% as a result of evaluating the worth at a fixed buckling  $B_z^2 = 6.11$  m<sup>-2</sup> instead of  $B_z^2(h_c^A)$  in the actual experiment. This happened in the 100%-voided core, but mostly such corrections were within the range of a few percent. The CR worth,  $\rho$ , at an arbitrary buckling,  $B_z^2$ , can be derived by using Eqs. (4) and (5) and the  $a$  value of Table II. Experimental uncertainty in  $B_z^2(h_c^A)$  is about

<sup>7</sup>C. R. RICHEY and T. J. OAKES, *Nucl. Sci. Eng.*, **47**, 40 (1972).

<sup>8</sup>M. UEDA, *J. Nucl. Sci. Technol.*, **12**, 229 (1975).

<sup>9</sup>Since the relations,  $\partial\rho/\partial h \propto 1/h^3$  and  $\Delta h \ll h_c$ , hold in the present work, the present first-order approximation is considered adequate.

TABLE III  
Critical Buckling and Reactivity Worth of CRs

| Core Number | Number of CRs | Position of CRs Loaded                              | Critical Axial Buckling, $B_z^2$ ( $m^{-2}$ ) |      |      |      |      | Worth in dollars, for $B_z^2 = 6.11$ ( $m^{-2}$ ) |      |      |      |       |  |
|-------------|---------------|---|---|------|------|------|------|---|------|------|------|-------|--|
|             |               |   | Coolant Void Fraction (%)                     |      |      |      |      | Coolant Void Fraction (%)                         |      |      |      |       |  |
|             |               |   | 0   | 30   | 70   | 86.7 | 100  | 0   | 30   | 70   | 86.7 | 100   |  |
| 1           | 0             |   | 8.67  | 8.37 | 7.54 | 7.30 | 6.11 |   |      |      |      |       |  |
| 2           | 1             | 1D1   | 7.92  | 7.65 | 6.83 | 6.65 | 5.49 | 1.51  | 1.45 | 1.69 | 2.07 | 2.23  |  |
| 3           | 1             | 3D1   | 8.02  |      |      |      | 5.59 | 1.29  |      |      |      | 1.89  |  |
| 4           | 1             | 3D3   | 8.12  |      |      |      | 5.67 | 1.08  |      |      |      | 1.60  |  |
| 5           | 1             | 1D5   | 8.22  | 7.94 | 7.12 | 6.92 | 5.73 | 0.90  | 0.85 | 1.00 | 1.28 | 1.37  |  |
| 6           | 1             | 3D5   | 8.27  |      |      |      | 5.78 | 0.79  |      |      |      | 1.19  |  |
| 7           | 1             | 5D7   | 8.50  | 8.20 | 7.38 |      | 5.95 | 0.34  | 0.33 | 0.40 |      | 0.58  |  |
| 8           | 2             | 1B1 + 1D1   | 7.32  | 7.06 | 6.26 |      | 5.00 | 2.70  | 2.64 | 3.07 |      | 4.05  |  |
| 9           | 2             | 3B3 + 3D3   | 7.43  |      |      |      | 5.08 | 2.48  |      |      |      | 3.73  |  |
| 10          | 2             | 1B5 + 1D5   | 7.59  | 7.33 | 6.52 | 6.35 | 5.21 | 2.15  | 2.09 | 2.44 | 2.99 | 3.24  |  |
| 11          | 2             | 5B7 + 5D7   | 8.29  | 8.01 | 7.19 |      | 5.77 | 0.76  | 0.71 | 0.84 |      | 1.23  |  |
| 12          | 2             | 1B1 + 1C1   | 7.44  |      |      |      | 5.08 | 2.46  |      |      |      | 3.74  |  |
| 13          | 2             | 1B3 + 1C1   | 7.35  |      |      |      | 5.02 | 2.63  |      |      |      | 3.97  |  |
| 14          | 4             | 1A1 + 1B1 + 1C1 + 1D1                               | 6.77  | 6.51 | 5.71 |      | 4.49 | 3.80  | 3.74 | 4.44 |      | 5.92  |  |
| 15          | 4             | 5A1 + 1B5 + 5C5 + 1B5                               | 6.19  | 6.01 | 5.26 |      | 4.12 | 4.85  | 4.76 | 5.54 |      | 7.34  |  |
| 16          | 4             | 3A3 + 1B3 + 1C1 + 3D1                               | 6.42  |      |      |      | 4.22 | 4.51  |      |      |      | 6.97  |  |
| 17          | 4             | 3A3 + 5B3 + 5C5 + 3D5                               | 6.60  | 6.33 | 5.53 |      | 4.37 | 4.15  | 4.11 | 4.86 |      | 6.40  |  |
| 18          | 5             | 3A3 + 5B3 + 1C1 + 3D5 + 5C5                         | 5.84  | 5.58 | 4.81 |      | 3.75 | 5.67  | 5.61 | 6.68 |      | 8.77  |  |
| 19          | 7             | 1B3 + 5B3 + 3D1 + 1C1 + 5C1 + 3D5 + 1C5             | 5.36  |      |      |      | 3.28 | 6.62  |      |      |      | 10.59 |  |
| 20          | 8             | 1B3 + 5B3 + 3D1 + 1C1 + 5C1 + 3D5 + 1C5 + 5C5       | 5.32  |      |      |      | 3.23 | 6.70  |      |      |      | 10.79 |  |
| 21          | 8             | 3A3 + 1B3 + 5B3 + 1C1 + 5C1 + 3D5 + 1C5 + 5C5       | 4.91  |      |      |      | 2.91 | 7.52  |      |      |      | 12.05 |  |
| 22          | 8             | 3A3 + 1B3 + 5B3 + 3D1 + 5C1 + 3D5 + 1C5 + 5C5       | 4.49  |      |      |      | 2.59 | 8.37  |      |      |      | 13.33 |  |
| 23          | 9             | 3A3 + 1B3 + 5B3 + 3D1 + 1C1 + 5C1 + 3D5 + 1C5 + 5C5 | 4.30  |      |      |      | 2.38 | 8.75  |      |      |      | 14.16 |  |

$\pm 0.07$   $m^{-2}$ , and relative errors of the reactivity measurements vary around 2.0 to 2.5%, depending on the void conditions.

The worths of the individual outer and inner annulus absorbers were measured at the position 1C1 (see Fig. 3) of the nonvoided core, and it was found that the worth for the outer one was smaller by only 2% than the regular double annulus, while that for the inner one alone was smaller by ~16%.

#### II.F. Flux Traverse

For cores having a multiple number of CRs, activation traverses were made by irradiating copper wires at the centers of the fuel clusters. Since the irradiation was done without any filters, these measurements include the effect of the epithermal neutrons. However, the relative activation shapes may be regarded as those by pure thermal neutrons within experimental accuracy, because the cadmium ratio of the copper wire

activity was in the range of ~18 to 22 all over the core. The results of these flux traverses are shown in Table IV.

### III. CALCULATION

#### III.A. Method of Calculation

The design calculation of the FUGEN CRs is based on the AA method.<sup>4</sup> Interference effect of multiple CRs is taken into the "absorption areas" by adopting the "controlled super-cell" model, and by applying a flat boundary condition at its outer surface. The direct full-core diffusion calculation applying the LD method at the surface of a CR requires much computer time when multiple CRs are inserted in various rod patterns. The LD method may be useful, however, as an alternative since it better reproduces the flux shape near the CRs. The procedure of the calculations is shown in Fig. 5. Three-group cell constants were ob-

TABLE IV  
Activation Traverse Data

| Core Number     | Coolant Void (%) | Relative Activation Rate at the Center of Fuel Cluster |      |      |      |      |      |      |      |      | Remarks and Statistical Error  |
|-----------------|------------------|--|------|------|------|------|------|------|------|------|--------------------------------|
|                 |                  | 8C8  | 6C6  | 4C4  | 2C2  | 0    | 2A2  | 4A4  | 6A6  | 8A8  |                                |
| 1               | 0,100            | 0.25   | 0.52 | 0.75 | 0.93 | 1.00 | 0.93 | 0.75 | 0.52 | 0.25 | Radial reflector saving: 15 cm |
| 9A <sup>a</sup> | 100              | 0.47   | 0.89 | 1.19 | 1.29 | 1.29 | 1.25 | 1.13 | 0.82 | 0.45 | 0.5%                           |
| 9B <sup>a</sup> | 100              | 0.36   | 0.64 | 0.66 | 0.87 | 1.29 | 0.86 | 0.65 | 0.62 | 0.33 | 0.5%                           |
| 18              | 100              | 0.37   | 0.52 | 0.79 | 0.93 | 1.11 | 1.20 | 1.15 | 1.18 | 0.63 | 0.5%                           |
| 22              | 0                | 0.15   | 0.24 | 0.34 | 0.59 | 0.77 | 0.79 | 1.15 | 1.27 | 0.65 | 0.7%                           |
|                 | 100              | 0.24   | 0.31 | 0.41 | 0.69 | 0.85 | 0.82 | 1.07 | 1.21 | 0.74 | 0.5%                           |
| 23              | 0                | 0.09   | 0.16 | 0.21 | 0.25 | 0.42 | 0.64 | 1.05 | 1.25 | 0.63 | 0.7%                           |
|                 | 100              | 0.19   | 0.25 | 0.29 | 0.34 | 0.51 | 0.72 | 1.07 | 1.24 | 0.77 | 0.5%                           |

<sup>a</sup>Two CRs were inserted in Core 9A at positions 3B3 and 3D3 and in Core 9B at positions 3A3 and 3C3.

tained by a METHUSELAH-II code.<sup>10-12</sup> It generates fluxes, reaction rates, group constants, multiplication factors, etc., of a cluster lattice in five energy groups (three fast and two overlapping thermal groups), and also in two groups (one fast and one thermal group).

In the CR analysis, three-group approximation is employed. The "fast group" is a collapse from the two fast groups covering the energy range of 10 MeV to 5.53 keV, and the epithermal group is the third group of the code.

It is assumed that the CR absorbs only epithermal and thermal neutrons. A controlled super-cell model is considered to obtain the linear extrapolation distances into the CR surface.

The super cell consists of four fuel assemblies with a CR in their center. The super cell is cylindrical and calculated by the one-dimensional transport codes THERMOS (Ref. 13) for thermal regions and DTF for epithermal regions.<sup>14</sup> To homogenize each annular region, the

atomic number density was adjusted in such a way as to conserve the effective reaction rate considering the fine structure of the thermal-neutron flux distribution.

In the case of a direct full-core diffusion calculation in X-Y coordinates by the LD method, the cylindrical CRs were converted to the effectively equivalent square rods, 6.95 × 6.95 cm in cross section, based on the Hurwitz proposal,<sup>3</sup> but with use of linear extrapolation distances calculated for the annulus.

<sup>10</sup>M. J. BRINKWORTH and J. A. GRIFFITHS, "METHUSELAH-II, A Fortran Program and Nuclear Data Library for the Physics Assessment of Liquid-Moderated Reactors," AEEW-R480, U.K. Atomic Energy Authority, Winfrith (1966).

<sup>11</sup>R. ALPIAR, "METHUSELAH-I, A Universal Assessment Programme for Liquid Moderated Reactor Cells, Using IBM 7090 or STRETCH Computers," AEEW-R135, U.K. Atomic Energy Authority, Winfrith (1964).

<sup>12</sup>M. J. BRINKWORTH, "METHUSELAH-III, A Fortran Program and Nuclear Data Library for the Physics Assessment of Liquid-Moderated Reactors," AEEW-R631, U.K. Atomic Energy Authority, Winfrith (1969).

<sup>13</sup>H. C. HONECK, "THERMOS, A Thermalization Transport Theory Code for Reactor Lattice Calculation," BNL-5826, Brookhaven National Laboratory (1961).

<sup>14</sup>B. G. CARLSON et al., "DTF Users Manual," UNC Phys/Math-3321, Vol. I, United Nuclear Corporation (1963).

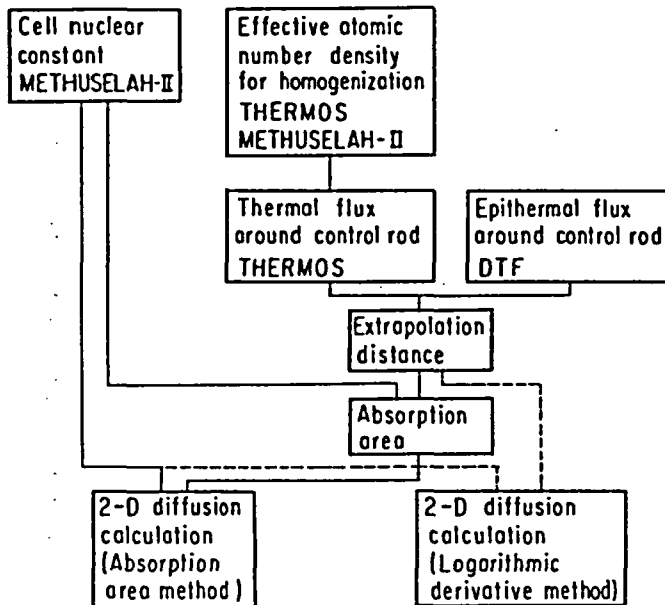


Fig. 5. Flow diagram of calculation.

### III.B. Linear Extrapolation Distances, $d_i$

The extrapolation distance,  $d_3$ , for thermal neutrons is estimated from the thermal flux distribution around the CR and the absorption rate in the CR. The total thermal-neutron absorption ( $\mathcal{R}_3$ ) in the CR annulus is equal to the integral neutron current into the annulus through the outer and inner surfaces. The linear extrapolation distances,  $d_3$ , into the CR annulus at both surfaces are assumed to be equal and are given by

$$d_3 = \frac{\lambda_{t3}}{3\mathcal{R}_3} (S_{out}\phi_{3out} + S_{in}\phi_{3in}), \quad (7)$$

where  $\lambda_{t3}$  is the transport mean-free-path, near the surface of the annulus, and  $S_{out}$  and  $S_{in}$  are the areas of the outer and inner surfaces, respectively.

The extrapolation distance,  $d_2$ , for epithermal neutrons is evaluated by considering the epithermal flux distribution, absorption rate, and slowing down rate around the CR. The total epithermal-neutron removal in the cylindrical CR ( $\mathcal{R}_2$ ) is the sum of the absorbed epithermal neutrons and the slowed down loss to the thermal group subtracting the slowed down gain from the fast group. It is equated to the epithermal-neutron current into the CR. The  $d_2$  is then given by

$$d_2 = \frac{\lambda_{t2}}{3\mathcal{R}_2} (S_{out}\phi_{2out}), \quad (8)$$

where  $\lambda_{t2}$  is the transport mean-free-path of epithermal neutrons in the outer medium.

### III.C. Absorption Areas, $A_i$

The total number of slowing down neutrons in the super cell is proportional to its area, and some fraction of slowed down neutrons is absorbed by the CR. The absorption area is therefore related to the total number of neutrons lost to the CR, and it is expressed in terms of the equivalent area of slowing down source neutrons. For the  $i$ 'th-group neutrons, it is given by

$$A_i = \frac{i\text{'th-group neutron absorption in the CR}}{\text{slowing down density into the } i\text{'th group}} \\ = -2\pi r_0 J_i(r_0) / \Sigma_s d_{i-1} \phi_{i-1}, \quad (9)$$

where  $r_0$  is the radius of the CR and  $-J_i(r_0)$  is the neutron current into the CR surface. To evaluate the  $A_i$ 's, it is assumed that

1. The fast neutrons are not absorbed by the CR and the slowing down source distribution to the epithermal group is flat.
2. The flux in the super-cell calculation is a function of the radial distance ( $r$ ) only.

Then, epithermal and thermal fluxes obey

$$\nabla^2 \phi_2 - (1/L_2^2)\phi_2 + Q/D_2 = 0 \quad (10)$$

$$\nabla^2 \phi_3 - (1/L_3^2)\phi_3 + (\Sigma_s d_2/D_3)\phi_2 = 0, \quad (11)$$

where  $L_2$  and  $L_3$  are the diffusion lengths for epithermal and thermal neutrons,  $D_2$  and  $D_3$  are the diffusion constants,  $\Sigma_s d_2$  is the slowing down cross section from epithermal group, and  $Q$  is the fast-neutron slowing down source. The boundary conditions applied for these equations are

1. the logarithmic-derivative boundary condition at the CR surface
2. the flat boundary condition at the outer boundary of the super cell.

The second condition expresses the shadowing effect of the adjacent CRs spaced uniformly.

The epithermal and thermal flux distributions obtained as solutions of Eqs. (10) and (11) yield the absorption areas for each group of neutrons:

$$A_2 = 2\pi r_0 L_2 [a(2) + d_2/L_2]^{-1}, \quad (12)$$

$$A_3 = \frac{2\pi r_0 L_3}{\epsilon} \left\{ \left[ \frac{L_2}{L_3} \left( 1 - \frac{L_3^2}{L_2^2} \right) \right]^{-1} [a(2) + d_2/L_2]^{-1} \right. \\ \left. + \zeta [a(3) + d_3/L_3]^{-1} \right\}, \quad (13)$$

where

$$\epsilon = 1 - a'(2) [a(2) + d_2/L_2]^{-1}, \quad (14)$$

$$\zeta = 1 - (1 - L_3^2/L_2^2)^{-1} [a(2) + d_2/L_2] [a(2) + d_2/L_2]^{-1} \\ (15)$$

$$a(i) = \frac{I_1(R_0/L_i)K_0(r_0/L_i) + K_1(R_0/L_i)I_0(r_0/L_i)}{I_1(R_0/L_i)K_1(r_0/L_i) - K_1(R_0/L_i)I_1(r_0/L_i)}, \quad (16)$$

$$a'(2) = \frac{I_1(R_0/L_2)K_0(R_0/L_2) + K_1(R_0/L_2)I_0(R_0/L_2)}{I_1(R_0/L_2)K_1(r_0/L_2) - K_1(R_0/L_2)I_1(r_0/L_2)}, \quad (17)$$

and where  $I_0$ ,  $I_1$ ,  $K_0$ , and  $K_1$  are the Bessel functions, and  $R_0$  is the radius of the super cell. Note that the shadowing effect of the adjacent CRs on the absorption areas depends mainly on the ratios,  $R_0/L_i$ . In the DCA experiment,  $R_0/L_2$  and  $R_0/L_3$  varied in the range from 2.7 to 3.9 and 2.7 to 2.9, respectively, as the void fraction varied. Therefore, the loss of absorption areas due to the shadowing effect of adjacent CRs is expected to be  $\sim 2\%$  at most. Absorption areas become relatively insensitive to the super-cell radius greater than a few diffusion lengths, and an example of such behavior is shown in Fig. 6.

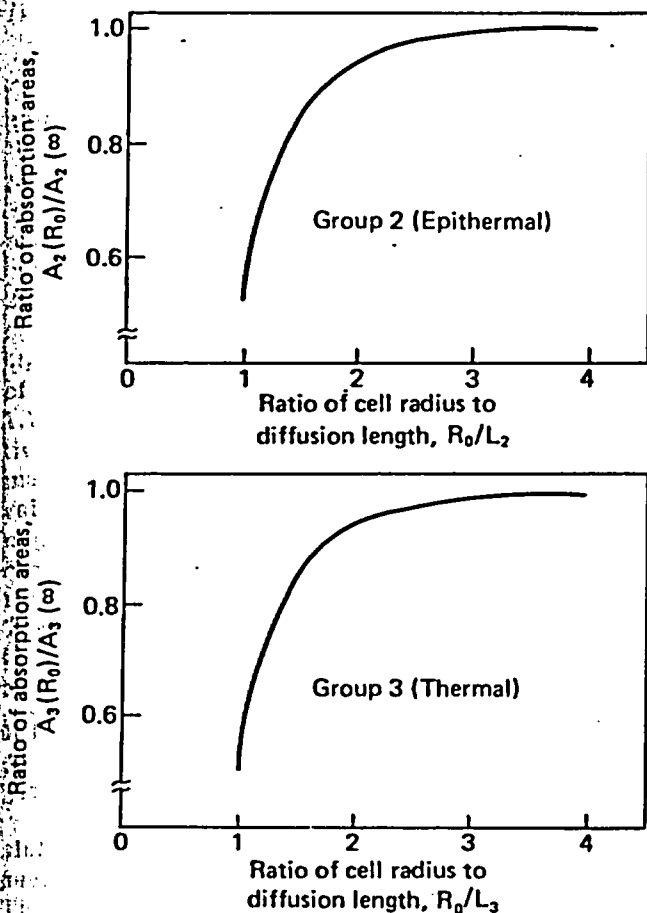


Fig. 6. Variation of absorption areas normalized to  $A_i(\infty)$  having no shadowing effect.

### III.D. Reactivity Calculation

The three-group diffusion equations in the reactor can be described in the forms

$$-D_1 \nabla^2 \phi_1 + \Sigma_{s1} \phi_1 + \Sigma_{a1} \phi_1 = \nu \Sigma_{f1} \phi_1 + \nu \Sigma_{f2} \phi_2 + \nu \Sigma_{f3} \phi_3, \quad (18)$$

$$-D_2 \nabla^2 \phi_2 + \Sigma_{s2} \phi_2 + \Sigma_{a2} \phi_2 = F_2 \Sigma_{s1} \phi_1, \quad (19)$$

$$-D_3 \nabla^2 \phi_3 + \Sigma_{a3} \phi_3 = F_3 \Sigma_{s2} \phi_2, \quad (20)$$

where

$$F_i = (A_c - A_i) / A_c, \quad (21)$$

and where  $A_c$  is the area of the super cell.

The last equation expresses the reduction rate of the slowing down source neutron to the  $i$ 'th energy group due to the CR in the super cell. If the flux distribution is represented using the super-cell buckling, i.e.,  $\nabla^2 \phi_i = -B_i^2 \phi_i$ , the reduced fission source in the following form also gives the correct multiplication factor, instead of adjusting slowing down source neutrons, i.e.,

$$\nu \Sigma_{f2} \rightarrow F_2 \nu \Sigma_{f2}, \quad (22)$$

$$\nu \Sigma_{f3} \rightarrow F_2 F_3 \nu \Sigma_{f3}. \quad (23)$$

In most of the present analyses, the "reduced fission sources" are used for the controlled super cell.

### III.E. Result of Calculation

The calculated results are shown in Table V as compared with the experiments. Although flux tilts were present in the DCA core as shown in Fig. 7, the calculations of reactivity worths using the AA method agreed with the experiments within about  $\pm 10\%$ , and the method seems simple and effective enough to predict the CR effects.

The disagreement between the AA method and the LD method can be explained as follows: Hurwitz assumed a black absorber model, whereas the actual absorber rods are rather gray to epithermal neutrons even though they might be considered black to thermal ones, and the effective "cylinder-to-square" conversion as proposed by Hurwitz does not seem sufficiently valid for epithermal neutrons. From the physical understanding, the logarithmic derivative boundary condition to the square edges of gray absorbers must become a more penetrative one, but this is not taken into account in the analysis of the present

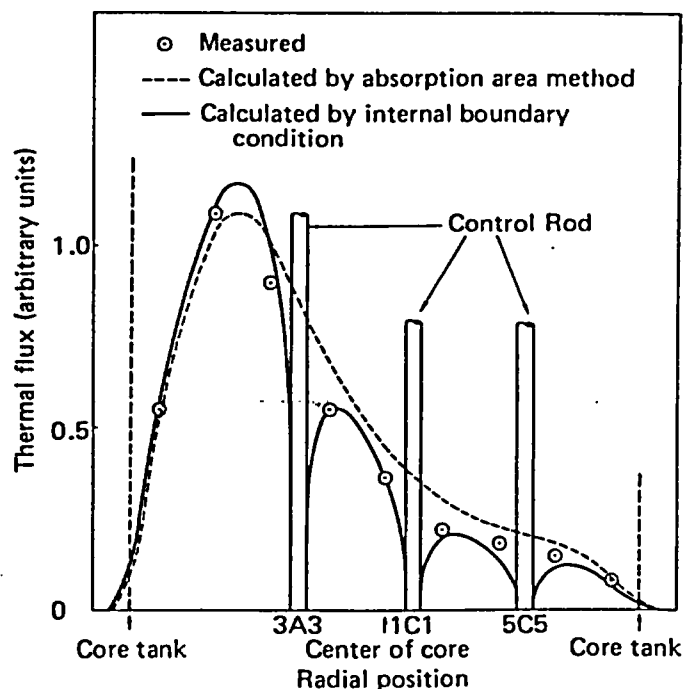


Fig. 7. Correlation of measured and calculated thermal flux shapes in the 0%-voided core with nine CRs fully inserted (see Table III, Core 23).

TABLE V  
 CR Worths

| Core Number | Number of CRs | Coolant Void Fraction (%) | Experimental Results (dollars) | Calculated Value (dollars) |                        |
|-------------|---------------|---------------------------|--------------------------------|----------------------------|------------------------|
|             |               |                           |                                | AA Method <sup>a</sup>     | LD Method <sup>b</sup> |
| 2           | 1             | 0                         | 1.51                           | 1.646                      | 1.875                  |
|             |               | 100                       | 2.23                           | 2.069                      | 2.394                  |
| 5           | 1             | 0                         | 0.90                           | 0.971                      | 0.986                  |
| 10          | 2             | 0                         | 2.15                           | 2.313                      | ---                    |
| 15          | 4             | 0                         | 4.85                           | 5.247                      | 5.578                  |
| 20          | 8             | 0                         | 6.70                           | 7.379                      | ---                    |
| 21          | 8             | 0                         | 7.52                           | 8.324                      | ---                    |
| 22          | 8             | 0                         | 8.37                           | 9.272                      | 9.658                  |
| 23          | 9             | 0                         | 8.75                           | 9.790                      | 10.058                 |
|             |               | 100                       | 14.16                          | 12.269                     | 13.742                 |

<sup>a</sup>Absorption area method.

<sup>b</sup>Diffusion calculation with logarithmic-derivative condition.

work and is suspected to be the reason for overestimating reactivity worths of the absorbers in the LD method compared to the AA method.

On the other hand, the AA method calculates a balance of neutron absorptions with a cylindrical absorber rod at the center of a super cell, and hence it seems to give a better reproduction of reactivity worth, but sacrifices the description of flux distribution close to the absorbers.

The CR worth in the voided core was found to be larger than that in the nonvoided core. This result is physically attributed to the larger diffusion area in the voided core.

An example of the calculated thermal-neutron flux distribution with nine control rods in the nonvoided core (Core 23) is shown in Fig. 7 together with the measurements. The agreement between the experiment and calculation was found reasonably good. The direct whole-core diffusion calculation with the logarithmic-derivative boundary conditions at the rod surface (LD method) yielded better flux distribution, although it required more computer time. Similar results were also observed in other cores with different control rod patterns.

#### IV. DISCUSSION

##### IV.A. Variation of CR Worth with Coolant Void Fraction

Table III shows that the CR worth increases, but the  $\Delta B_z^2$  value decreases, as the coolant void fraction increases. Neither the position nor the

number of CRs is sensitive to these results. The coolant-void dependence of CR worth can be interpreted by a two-group CR theory by Weinberg et al.<sup>15</sup>

With a slight rearrangement of the formula given in Ref. (15), the central CR worth is given by

$$\rho = (a/2\pi^2)\Delta B_z^2, \quad (24)$$

$$\begin{aligned} \Delta B_z^2 = & (7.5/R^2)[0.116(1 + \tau/L^2) \\ & + (\tau/L^2)\ln(L\sqrt{\tau}/MR_{eff}) \\ & + \ln(R/2.405 R_{eff})]^{-1}, \quad (25) \end{aligned}$$

where  $R$  is the effective core radius (155 cm in the DCA core) and  $R_{eff}$  is the effective radius of CR (3.5 cm in the present study). The CR is assumed to be black to thermal neutrons, but transparent to fast ones. A numerical study showed that the experimental  $a$  value, including anisotropy of  $M^2$ , reproduced the void dependence of CR worth very well, but the calculated  $a$  value, which neglects the anisotropy of  $M^2$ , did not. Equation (25) reproduced the void dependence of  $\Delta B_z^2$  satisfactorily by employing the calculated  $\tau$  and  $L^2$  given above. Equation (24), with the calculated  $a$  value, overestimated the CR worth by ~10% in the nonvoided core and underestimated it by ~20% in the 100%-voided core.

<sup>15</sup>S. GLASSTONE and M. C. EDLUND, *The Elements of Nuclear Reactor Theory*, p. 325, D. Van Nostrand Co., Inc., New York (1952).

#### IV.B. Estimation of Anisotropy of Migration Area, $M^2$

As discussed in the preceding section, the anisotropy of  $M^2$  may play an important role in the CR-worth evaluations. In the two-group approximation, the  $a$  value at criticality is given by Eq. (6). The values of  $k_{\infty}^*$  and  $M^2$  (isotropic) were experimentally determined elsewhere.<sup>8</sup> The calculated  $k_{\infty}^*$  was higher than the experiment by 1 to 2.5%, and the calculated  $M^2$  agreed with the experiment  $M^2$  (isotropic) within  $\pm 7\%$ . The ratio  $M_z^2/M^2$  can be calculated from Eq. (6). The values of  $M_z^2/M^2$  obtained in this manner are 0.95 and 1.16 for the cores of 0 and 100% voids, respectively. Since the isotropic value of  $M^2$  is estimated to have uncertainty of about  $\pm 6\%$ , and the  $a$  value of  $\pm 1.5$  to  $2\%$ , and since the value of  $\beta_{\text{eff}}$  might have some systematic uncertainties, the  $M_z^2/M^2$  evaluated in this way may not yet be well refined for a precise study of migration isotropy. The  $M_z^2/M^2$  value, however, is useful to interpret the difference of CR worth between experiment and calculation; but no corrective method is yet established to evaluate such an isotropy effect.

#### IV.C. Change of Reactivity due to Changes in Delayed Neutron Parameters

Delayed neutron parameters (DNPs) play essential roles in the determination of reactivity. The values of  $\beta_{\text{eff}}$  employed here were 0.00725, 0.00723, 0.00723, 0.00726, and 0.00732 for the cores of 0, 30, 70, 86.7, and 100% voids, respectively. These were obtained by using the DNPs in Refs. 16, 17, and 18, the self-shielding factor of gamma rays in the fuel cluster,  $F_\gamma = 0.23$ , in Ref. 19, effectiveness factors  $\gamma$ 's for delayed and photodelayed neutrons calculated with use made of the Gwin formula,<sup>20</sup> and experimental  $^{235}\text{U}$  in Ref. 21. The slight variation in  $\beta_{\text{eff}}$  with coolant void fraction was due mostly to considerable variation in the  $^{235}\text{U}$  value, since  $\gamma$  ranged between 1.01 and 1.03 and was insensitive to the void fraction.

The DNPs have been reevaluated extensively in recent works. Among such studies, the DNP sets by Tomlinson,<sup>22</sup> Evans-Thorpe-Krick (ETK),<sup>23</sup> and

<sup>16</sup>G. R. KEEPIN, T. F. WIMETT, and R. K. ZEIGLER, *Phys. Rev.*, **107**, 1044 (1957); see also G. R. KEEPIN, *Physics of Nuclear Kinetics*, p. 73, Addison-Wesley Publishing Co., Inc., Reading, Massachusetts (1965).

<sup>17</sup>S. BERNSTEIN, W. M. PRESTON, G. WOLFE, and R. E. SLATTERY, *Phys. Rev.*, **71**, 573 (1947).

<sup>18</sup>W. K. ERGEN, "Hard Gamma Emitters among Fission Fragments," ANP-59, Oak Ridge National Laboratory (1951).

<sup>19</sup>Y. KANEKO, *J. Nucl. Sci. Technol.*, **8**, 34 (1971).

<sup>20</sup>"Reactor Physics Constants," ANL-5800, 2nd ed., p. 443, Argonne National Laboratory (1963).

<sup>21</sup>H. SAKATA, Y. HACHIYA, K. SHIBA, N. FUKUMURA, and A. NISHI, *Trans. Am. Nucl. Soc.*, **16**, 267 (1973).

Cox<sup>24</sup> were examined, and the extent of their influence to the evaluated CR worths (dollar and  $\Delta k/k$  units) were studied. The result of such investigations were that both the Tomlinson and the ETK sets resulted almost in the same dollar reactivities as those shown in Table III, but the dollar reactivities from the Cox set were smaller by 2%. Both the ETK and the Cox values resulted in larger  $\Delta k/k$  reactivities by 3.5%, and the Tomlinson results were larger by 4.2% than the evaluations based on Keepin<sup>16</sup> and others.<sup>17,18</sup> These numerical examinations show that the DNPs may possibly cause an inevitable uncertainty in the experimental reactivity worth evaluations.

#### V. CONCLUSION

A series of CR experiments was performed in a heavy-water-moderated, pressure-tube-type critical facility, DCA, to study the physics of the annular CRs to be used in the FUGEN reactor. Reactivity worths of the CRs were determined from the difference of the critical core heights with and without the CRs. Flux traverse measurements were made in various core configurations. The experiment was carried out by changing the CR patterns, and void fraction of coolant in the cores of 1.2%-enriched  $\text{UO}_2$  lattices of 28-pin clusters in square arrays spaced at 22.5 cm. Anisotropy of migration area,  $M_z^2/M^2$ , was estimated from a series of measurements to understand the possible causes resulting in the difference of the CR worth between experiment and calculation.

Calculations were mostly done by the AA method, which was employed in the design calculation of the FUGEN CRs. Although flux tilts were present in the DCA core as shown in Fig. 7, the calculation of the CR worth agreed with the experiments within  $\pm 10\%$ . The calculation tended to somewhat overestimate the worth in the 0%-voided core and underestimate it in the 100%-voided core. This tendency was greatly improved by taking the anisotropy of migration area  $M^2$  into consideration. The AA method calculations were supported by the direct full-core diffusion calculations applying the LD method at the surface of the CR. The LD method predicted better flux shape near the control rods, but slightly poorer CR worths.

<sup>22</sup>L. TOMLINSON, "Delayed Neutrons from Fission—A Compilation and Evaluation of Experimental Data," AERE-R6993, U.K. Atomic Energy Research Establishment, Harwell (1972).

<sup>23</sup>A. E. EVANS, M. M. THORPE, and M. S. KRICK, *Nucl. Sci. Eng.*, **50**, 80 (1973).

<sup>24</sup>S. A. COX, "Delayed Neutron Data—Review and Evaluation," ANL/NDM-5, Argonne National Laboratory (1974).

## APPENDIX

TWO-GROUP REACTIVITY COEFFICIENT  
OF MODERATOR

The two-group critical equations for a single-region reactor with leakages in the  $r$  and  $z$  directions are

$$\left. \begin{aligned} (\Sigma_{s1} + \Sigma_{a1} + D_{1r}B_r^2 + D_{1z}B_z^2)\phi_1 \\ = (\nu\Sigma_{f1}\phi_1 + \nu\Sigma_{f2}\phi_2)/k_{eff} \\ (\Sigma_{a2} + D_{2r}B_r^2 + D_{2z}B_z^2)\phi_2 = \Sigma_{s1}\phi_1 \end{aligned} \right\} \quad (A.1)$$

where notations are all conventional.

The  $k_{eff}$  obtained from these equations is

$$k_{eff} = k_{\infty 2}^* / [(1 + \tau_r B_r^2 + \tau_z B_z^2)(1 + L_r^2 B_r^2 + L_z^2 B_z^2)] \quad (A.2)$$

where

$$\left. \begin{aligned} k_{\infty 2}^* &= \eta f \cdot p \cdot E \\ \eta f &= \nu\Sigma_{f2}/\Sigma_{a2} \quad , \quad p = \Sigma_{s1}/(\Sigma_{s1} + \Sigma_{a1}) \\ E &= 1 + (1/\eta f)(\nu\Sigma_{f1}/\Sigma_{s1})(1 + L_r^2 B_r^2 + L_z^2 B_z^2) \\ \tau_r &= D_{1r}/(\Sigma_{s1} + \Sigma_{a1}) \quad , \quad L_r^2 = D_{1r}/\Sigma_{a2} \\ \tau_z &= D_{1z}/(\Sigma_{s1} + \Sigma_{a1}) \quad , \quad L_z^2 = D_{1z}/\Sigma_{a2} \end{aligned} \right\} \quad (A.3)$$

If one considers the case that the axial buckling is slightly increased from  $B_{zc}^2$  to  $B_z^2 (= B_{zc}^2 + \Delta B_z^2)$ ,

thereby keeping the constant radial buckling  $B_r^2$ , the  $k_{\infty 2}^*$  is obtained from Eq. (A.2) by setting  $k_{eff} = 1.0$ , and the reactivity change in dollar unit  $\Delta\rho$  becomes

$$\beta_{eff}\Delta\rho = 1 - 1/k_{eff} = \frac{M_z^2 \Delta B_z^2}{k_{\infty 2}^*} \times \left[ 1 + \frac{L_r^2 \tau_z + \tau_r L_z^2}{M_z^2} B_{rc}^2 + \frac{\tau_z L_z^2}{M_z^2} (B_{zc}^2 + B_z^2) \right] \quad (A.4)$$

The value in the brackets of Eq. (A.4) lies between 1.0 and 1.1 in the present work. That fact allows us to neglect the anisotropy effect of  $\tau$ ,  $L^2$ , and  $M^2$  described in the blanket. The  $B_z^2$  is nearly equal to  $B_{zc}^2$ , and Eq. (A.4) becomes

$$\beta_{eff}\Delta\rho = \frac{M_z^2 \Delta B_z^2}{k_{\infty 2}^*} \left( 1 + 2 \frac{\tau L^2}{M^2} B_c^2 \right) \quad (A.5)$$

The  $\Delta\rho/\Delta h$  value, expressed by Eqs. (5) and (6), is obtained from Eq. (A.5) by assuming a cosine shape of axial flux.

## ACKNOWLEDGMENTS

The authors are indebted to Mr. H. Sakata and Mr. H. Kikuchi of the Power Reactor and Nuclear Fuel Development Corporation for valuable discussions and suggestions. Thanks are also expressed to the staffs of DCA Laboratory for assistance in carrying out the experiments.